ACS Catalysis

RESEARCH ARTICLE

pubs.acs.org/acscatalysis

Catalytic Reduction of Hexavalent Chromium Using Flexible Nanostructured Poly(amic acids)

Marcells A. Omole, Veronica A. Okello, Vincent Lee, Lisa Zhou, and Omowunmi A. Sadik*

Department of Chemistry, Center for Advanced Sensors & Environmental Systems (CASE), State University of New York at Binghamton, P.O. Box 6000, Binghamton, New York 13902, United States

Christopher Umbach

Department of Materials Science & Engineering, Cornell University, 126 Bard Hall, Ithaca, New York 14853-1501, United States

Bahgat Sammakia

Department of Mechanical Engineering, Center for Advanced Microelectronics Manufacturing, State University of New York at Binghamton, P.O. Box 6000, Binghamton, New York 13902, United States

Supporting Information

ABSTRACT: Conducting polymers can be tuned by manipulating the delocalized π electron system for chemical and electrocatalytic applications. We hereby describe the reduction of Cr(VI) to Cr(III) by flexible nanostructured conducting poly(amic acid) (PAA) in both solution phase and as a thin film on a gold electrode. Sodium borohydride was used as a reducing agent to prepare different sizes (3−20 nm) of palladium nanoparticles (PdNPs). The effects of experimental parameters such as particle size, temperature, and Cr(VI) concentration on the kinetics and efficiency of reduction process were investigated. Results show that in PAA solution, Cr(VI) was efficiently reduced by 85.9% within a concentration range of 1.0×10^{-1}−1.0×10^{2} mM. In the presence of PdNPs and heat (40 °C), the reduction efficiency increased to 96.6% and 99.9% respectively. When employed on a solid electrode, PAA undergoes a quasi-reversible electrochemistry in acidic media with reduction efficiency for Cr(VI) at 72.84%. The method was validated using both colorimetric and Electron Paramagnetic Resonance techniques, which confirmed the formation of Cr(III) as the product of catalytic reduction. Additional characterization conducted using transmission electron microscopy (TEM), X-ray diffraction (XRD), and X-ray photoelectron spectroscopy (XPS) confirmed that there was no significant change in Pd particle size and distributions after dispersion in PAA whereas its phase and oxidation state remained unchanged. Electrochemical characterization showed the reversible and recyclable features of PAA thus confirming its dual role as catalyst stabilizer and reducing agent. This approach provides a significant advantage over conventional methods such as bioremediation which typically require longer time for complete reduction.

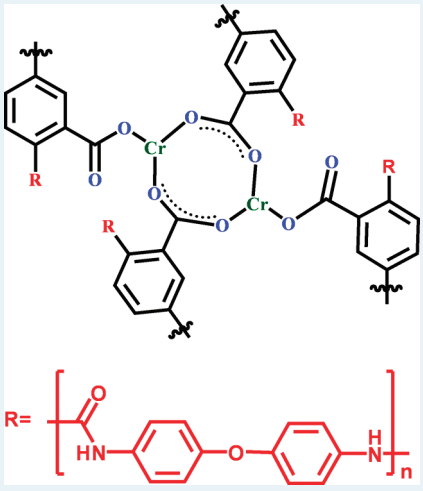

KEYWORDS: poly(amic) acid, Pd, nanoparticles, reduction, catalyst, hexavalent chromium

INTRODUCTION

Hexavalent chromium [Cr(VI)] is a well-known carcinogen and highly mobile in the environment while Cr(III) can be readily precipitated or adsorbed as $Cr(OH)_3$ by organic and inorganic substrates at neutral pH.[1,2] An effluent containing Cr(VI) results in negative impact on human health and the environment, and 0.1 mg L^{-1} is the permissible level in wastewater.[1−4] Chromate is a significant groundwater contaminant at the U.S. Department of Energy (DOE) Hanford Site in southeastern Washington (WA) state and is also one of the major components of nuclear wastes at this site.[5,6] It negatively impacts on the quality of the vitrification products by making them less stable. In other words Chromium can interfere with the High Level Waste (HLW) immobilization process by forming spinel phases in the melter[6]. These spinels (group of oxides having similar structures) adversely affect the melter performance by

Received: October 5, 2010
Revised: December 14, 2010
Published: January 18, 2011

accumulating as solid phases separate from the molten glass, leading to pouring difficulties, cold cap freezing, and foam stabilization.[4−6] For this reason and other related environmental effects, there is an urgent need to develop practical, low cost techniques to ensure safe disposal of chromium in the much less toxic and less mobile trivalent form, Cr(III), into the environment.

Current approaches for removing Cr(VI) from the environment include chemical precipitation, ion exchange, reverse osmosis, membrane processes, evaporation, solvent extraction, and adsorption among others.[7−9] An area of expanding research toward Cr(VI) reduction in the environment is its complexation with conducting polymeric materials and subsequent conversion to the less toxic form.[2,10−23] The unique properties of conducting polymers and their use for the reduction of Cr(VI) to Cr(III) were first reported in 1993[10] using electrochemically synthesized polypyrrole films. The advantages of conducting polymers for Cr(VI) reduction compared to conventional reducing agents such as the sulfur compounds (FeS, S/PdNPs,)[2,11] are that the reduction process is reversible and the conducting polymers could be recycled (Supporting Information, Figure 1). However, one of the limitations of polypyrrole is the loss of its electrochemical activity after consecutive cycles under open circuit conditions.[11]

Recent studies in our laboratory[1−3] have shown that elemental sulfur and formic acid in the presence of palladium nanoparticles catalyst are capable of transforming hexavalent chromium Cr(VI) into the much less toxic and less mobile trivalent form, Cr(III). However, it has been reported that Pd particles often suffer from sulfur poisoning following adsorption of sulfur atoms onto their surfaces, thus reducing their catalytic activity.[5] Formic acid on the other hand, is dangerously irritating to the skin, eyes, and mucous membranes and may also be toxic to the kidneys. Atmospheric concentrations as low as 32 mg/L may be corrosive; the EPA has specifically listed formic acid as a hazardous waste under RCRA and has been assigned EPA Hazardous Waste No. U123.[24] Even though these remediation methods have proved efficient and effective in reducing Cr(VI) in both water and soil, there is an increasing interest to use greener methods and to simplify the detection approaches via speciation, complexation, and sensitive detection.

The present work focuses on the reduction of Cr(VI) using flexible polyamic acid as reducing agent. PAA is a conducting electroactive polymer, and its properties can be tuned by manipulating the delocalized π electron system for chemical and electrocatalytic applications. PAA provides a means of generating nanocomposites containing monodispersed metal particles while retaining its physical and chemical properties. It is versatile in both organic and inorganic solvents because of its chemical resistance.[25,26] The carbonyl and amide functionalities in polyamic acids act as anchors resulting in the fabrication of flexible nanostructured polyamic acid-silica (PSG) films. In this work, we report the development of a novel palladium nano-PAA material that efficiently reduces Cr(VI) to Cr(III) in solution and in the solid phase, hence acting as a catalyst, reducing and stabilizing agent in the preparation of palladium nanoparticles. PAA is a conducting polymer that is easy to synthesize, mechanically stable, and a suitable material for Cr(VI) reduction. This is because metal nanoparticles can be incorporated into PAA, and the resulting matrixes have been shown to act like redox polymers. Unlike polyimides, PAA has significantly higher cation-complexing properties because of the presence of both carboxylic acid and amide functionalities.[25,26] To the best of our knowledge, we are not aware of any prior work in which polyamic acids have been used for the catalytic reduction, detoxification, or immobilization of Cr(VI).

EXPERIMENTAL SECTION

Materials. All chemicals were either reagent or analytical grade and were used as received from the vendors without further purification. 100% *N*,*N*-Dimethylformamide (DMF), sodium acetate trihydrate, sodium borohydride, ammonium sulfate, potassium phosphate, and calcium nitrate were purchased from Fisher Scientific, Fair Lawn, NJ. Potassium chromate, magnesium sulfate, potassium chloride, glacial acetic acid, sodium phosphate dibasic, sodium phosphate monobasic, and concentrated sulfuric acid were purchased from J.T. Baker Chemicals Co., Phillipsburg, N.J. Palladium acetate, 4,4′-oxidianiline (ODA), triethylamine (TEA), pyromellitic dianhydride (PMDA), and sodium acetate were purchased from Sigma Aldrich, Milwaukee, WI.

Stock Solutions. Unless otherwise stated, all reagents were prepared using Nanopure water with resistivity of 18.0 MΩ cm. Cr(VI) was prepared by dissolving 1.94 mg of potassium chromate in 1.00 L of Nanopure water. Phosphate Buffer saline 0.01 M (PBS) was prepared by dissolving 1.92 g of $Na_2HPO_4 \cdot 7H_2O$, 0.3416 g NaH_2PO_4, and 8 g of NaCl in 1.00 L nanopure water, and the pH adjusted using concentrated phosphoric acid or 10 M NaOH. Acetate buffer was prepared by dissolving 0.238 g of sodium acetate trihydrate in 1.00 L nanopure water, and its pH adjusted to 3 and 6 using glacial acetic acid. One M Cr(VI) stock solution was prepared by dissolving 7.36 g of potassium dichromate in deionized water in a 25 mL standard flask.

Instrumentation. An HP 8453 UV−visible diode array spectroscopy system was used for absorption measurements. Electrochemical measurements were performed using a BAS potentiostat/galvanostat Model 100B (Princeton, NJ) equipped with a gold working electrode, a Pt counter electrode, and a Ag/AgCl/1 M KCl (sat) reference electrode (Bioanalytical Systems Inc., West Lafayette, IN). All potentials were measured versus the Ag/AgCl as reference. All data collection and analysis were carried out using Model 270/250 Research Electrochemistry Software 4.30. X-ray powder diffraction (XRD) data was collected on a Scintag XDS2000 0-0 powder diffractometer equipped with a Ge(Li) solid-state detector and CuKα sealed tube (λ = 1.54178 Å). X-ray photoelectron spectroscopy (XPS) PHI 5000 versaProbe ULVAC-PHI, inc with monochromatic Al Kα (1486.7 eV) was used for surface analysis. Electron Paramagnetic Resonance spectrometer (Bruker EleXsys E680 EPR spectrometer) with its field set at 3480 G was used for confirmation of presence of Cr(III) in the reaction product.

Synthesis of Polyamic Acid. Synthesis of PAA was carried out as described elsewhere[25] (Supporting Information, Scheme 1). The preparation procedure involves the following steps: 2.01 g of ODA plus 42 mL of DMF were stirred in a 0.50 L round-bottom flask. PMDA powder (2.18 g) was added to the solution for over 1 h. MeOH (35.0 mL) containing 0.020 mols of TEA was then added. The solution was stirred for 24.0 h, resulting in a yellow viscous solution of PAA. The solid content of the resulting PAA was 9.80%. This viscous PAA was soluble in phosphate-buffered saline (PBS).

Table 1. Experimental Setup

	1000 mM Cr(VI) (mL)	H_2O (mL)	TEA in MeOH (mL)	final conc. (μM)	PAA (mg)	PdNPs (mg)
reaction(I)	10.0	5.0	5.0	0.500	0.0	0.0
reaction(II)	10.0	5.0	5.0	0.500	1.5	0.0
reaction(III)	10.0	5.0	5.0	0.500	1.5	1.5

Synthesis of Palladium Nanoparticles. Palladium nanoparticles were synthesized as reported in literature.[1,27] To tune the surface of the PdNPs for efficient catalytic reactions, the dried Pd particles were reconstituted to 3.00 mg/mL in a mixture of PAA and acetate buffer (pH 3.00) to generate a fresh colloidal suspension of the palladium nanoparticles. The following amounts of PdNPs-to-PAA by mass per mL were redispersed in DMF: (a) 1:1, (b) 3:1, and (c) 5:1. Depending on the amount of sodium borohydride used, different sizes of colloidal PdNPs were regenerated (Supporting Information, Figure 1 A−C).

TEM Studies of Palladium Colloids. Transmission electron microscopy (TEM) was performed on a Hitachi H-7000 Electron Microscope at 100 kV. The reaction medium was diluted 1:1 with the same solvent (DMF). A 10.0 μL portion of this solution was introduced onto a carbon-coated copper grid and allowed to evaporate at ambient conditions. The nanoparticle size distribution for each sample was determined by counting the size of approximately 300 palladium nanoparticles from several TEM images obtained from different places on the grids.

XRD and XPS Studies. Prior to XPS and XRD characterization, redispersed PdNPs in PAA were completely dried in an oven at 37 °C and ground into powdered form using a mortar and pestle. In case of XRD, the resulting powdered sample was put into a sample holder and inserted into the XRD instrument. 2θ values were taken from 30° to 80° at a step size of 0.5° per second. The experiment was performed under room temperature conditions. XPS studies of Palladium colloids were performed under ultra high vacuum conditions using monochromatic Al Kα X-rays which have limited penetrating power in a solid on the order of 1−10 μm. The data was referenced with adventitious carbon at 284.8 eV, 45.0° take off angle, and pass energy of 187.85 eV and 23.50 eV for survey and high resolution scans, respectively. Percentage concentration of each element and binding energies were then determined.

Control Experiments. Control reactions were carried out in a 100 mL reaction vessel containing 5.00 mL of acetate buffer. Briefly, 5.00 mL of TEA (0.02 mol) in MeOH was introduced into a vessel containing 1.50 mg of PAA followed by an addition of Cr(VI) and PdNPs where applicable. Table 1 shows a summary of the detailed experimental setup. In all cases the final concentration of Cr(VI) was 0.500 μM.

Reactions I and II were carried out at 40 °C and at pH 7.0 for a period of 14 min. Changes in the intensity of the absorption peak of Cr(VI) were monitored at a wavelength of 350 nm and comparison was made with standard Cr(VI) to estimate its final concentration. Percentage reductions in Cr(VI) concentration was recorded in each case.

Electrode Surface Preparation. Gold electrodes were first polished with alumina slurry (1.0 alpha micrometer and 0.05 gamma micrometer), rinsed with methanol and triply distilled water, before being sonicated in Piranha solution (3:1 mixture of concentrated H_2SO_4 and H_2O_2) for 15 min. The resulting surface was dried with a nitrogen stream after rinsing with ultra pure water. Gold electrode surfaces were coated with a layer of PAA by dropping 0.60 μL of the PAA solution on the electrode surface. This was repeated in triplicate at an interval of 3.00 h and was left to dry at ambient temperatures. PAA-covered gold electrodes were gently rinsed in ultra pure water and dried in a stream of nitrogen before use.

Reduction of Cr(VI) Using Flexible Polyamic Acid. Polyamic acid was used for reduction of Cr(VI) in aqueous phase. 1 M Cr(VI) stock solution was prepared by dissolving 7.36 g of potassium dichromate in deionized water in a 25 mL standard flask. Different concentrations of the working solutions were prepared by appropriate dilution with deionized water. To the different concentrations of Cr(VI) solution, PAA in powdered form was added and the mixture stirred at 300 rpm. The same procedure was repeated with the introduction of PdNPs into the reaction vessel. The products of the reaction were prepared for UV−vis analysis by a 1:20 dilution using acetate buffer solution (pH 3.00) after the PAA/PdNPs precipitates had been filtered. Optical absorption spectra were measured on a Hewlett-Packard model 8453 spectrophotometer at a fixed wavelength of 350 nm (the characteristic absorption peak for Cr(VI)). Prior to the spectrochemical analysis, a blank spectrum acetate buffer (pH 3.00) was taken. The concentration of Cr(VI) in solution was then recorded after different exposure times to both PAA and PdNP respectively. The electrochemical reduction was carried out on a PAA modified gold working electrode following the physical adsorption of the polymer onto the solid electrodes. Unless specified otherwise, all electrochemical measurements were carried out within a potential of −500 mV to +1000 mV versus Ag/AgCl in 1.00×10^{-3} M HCl at pH 3.00. The number of moles of Cr(VI) removed was calculated as the difference in the number of moles of the dichromate before and after treatment with PAA or PAA/PdNPs composites.

The concentration of Cr(VI) was calculated from the calibration curves constructed with absorbance of standard solutions in the range 1.00×10^{-2}−1.00×10^{5} mM. The efficiency of reduction reaction was calculated according to eq 1:

$$E_R = 100\,\frac{(C_0 - C_t)}{C_0} \qquad (1)$$

Where C_0 is the initial concentration of Cr(VI) in solution and C_t is the concentration of Cr(VI) after a specified exposure time (t) to polyamic acid powder or a polyamic acid modified Au-electrode.

RESULTS AND DISCUSSION

Particle Size and Morphology. The mean particle diameter recorded ranged from ≈3.00 to 20.0 nm with 9 nm being the dominant size as summarized in the TEM data in Supporting Information, Figure 1. The largest PdNPs colloids with an average size of 19 nm (Supporting Information, Figure 1-A) were obtained when 5 mg of sodium borohydride was used to reduce 3 mg of palladium acetate in 1 mL of DMF. We tested the ability of the PAA to redisperse the particles by redissolving the nanoparticles in different amounts of PAA in DMF. A better dispersion was observed for high PAA loading at 6.00 mg/mL. The ratios by mass/mL of PAA/PdNPs used were 1:1, 3:1, and 5:1. This result supports previous reports that the choice of reducing agent and experimental conditions provide a means of preparing colloidal nanoparticles with varying particle sizes.[28]

dx.doi.org/10.1021/cs100034z |ACS Catal. 2011, 1, 139–146

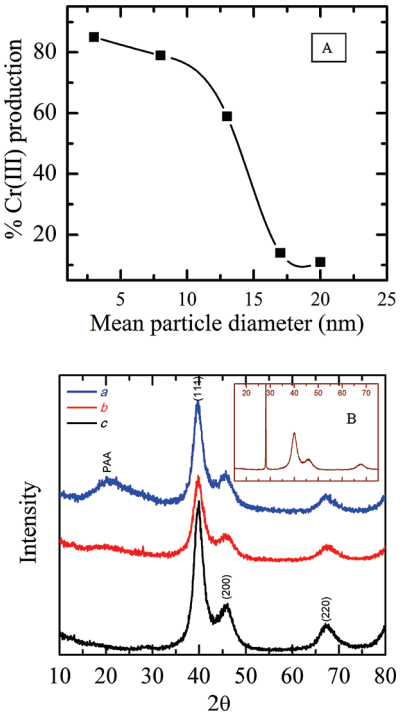

Figure 1. [A] Relation between Cr(III) produced and nanoparticles size determined for palladium colloids prepared by reduction with $NaBH_4$ and dispersed using PAA as a stabilizer. [B] XRD pattern of PdNPs after dispersion in PAA[a-1:1, b-3:1, c-5:1 PdNPs:PAA]; inset, XRD pattern of PdNPs before dispersion in PAA.

Catalytic Reaction, Stability, and Phase Changes. As reported previously,[28] the nanoparticle size and shape and the molecular weight of the protecting polymer influence the yield of the reaction.[29] The latter has been attributed to the extent to which the polymer interacts with the nanoparticles. Figure 1 A clearly shows that the yield of the product in the reduction of Cr(VI) to Cr(III) depends on the average nanoparticle size.

Even though other polymers and salts are generally considered stabilizers for most novel metal nanoparticles, some authors have reported undesirable palladium colloid aggregation during catalytic reactions carried out in such media.[2,30,31] PAA adequately disperses the inorganic nanoparticles (Pd) by encapsulation in the π-conjugated system. The advantages of using PAA is attributed to the electronic structure of the polymer chain, which strongly influences the characteristics of embedded metal nanoparticles thereby serving as potential novel catalysts. The π-conjugated polymer possibly provides an efficient route for shuttling electronic charge to the catalyst centers. The relation is nonlinear for averagely small and larger nanoparticles as the yield of Cr(III) in the reduction was 11% for the larger particles (average 19 nm) and 85% for the small particles (3.00 nm). Thus the catalytic activity is significantly affected by the average size of the Pd^0 particles and the amount of the protecting polymer (PAA) used (Figure 1 A).

XRD analysis of the composite materials was performed to determine the chemical state of PdNPs incorporated within the PAA membrane. The XRD patterns of PdNPs after dispersion in PAA are shown in Figure 1B. The procedures for the XRD analysis are detailed in the Experimental Section. PdNPs have a face centered cubic structure with *hkl* values of (111), (200), and (220). The diffractograms exhibit the peaks characteristics of crystalline metallic state for Pd. The full width at half-maximum (fwhm) of the strongest characteristic reflection (111) and (220) was used to estimate the average crystallite size by applying the Scherrer equation: [$D_p = 0.94\lambda/\beta_{0.5} \cos\theta$; where D_p is the crystallite size, $\beta_{0.5}$ is fwhm, and θ is the peak position]. The average crystallite sizes calculated from the (111) and (220) planes were found to be 3.82 nm before dispersion in PAA. There was no significant change in nanoparticle size after dispersion in PAA (3.58, 3.42, and 3.78 nm for 1:1, 3:1, 5:1 PdNPs/PAA respectively). The XRD amorphous pattern of PAA is as shown in the Supporting Information, Figure 3. The values of the lattice constant were calculated from the corresponding (111) and (200) planes on the XRD patterns. The lattice constant of PdNP was 3.905 Å. These are consistent with the standard values of Pd (a = 3.889 Å), given by the PDF file no. 7440053 and Au (a = 4.078 Å) in PDF file no. 040784, respectively.

The XPS spectrum of PAA-Pd was collected to determine the composition of the mixture and the possible oxidation state(s) of the Pd atoms. The material was pressed against soft indium foil and then analyzed at a base pressure of 1×10^{-10} Torr. Survey and high resolution scans were collected at specific pass energies (187.85 and 23.50 eV, respectively). The high-resolution spectra for the C1s, Pd3d5-Pd3d3-Pd3d, O1s, and N1s signals were collected in this mode to measure the accurate binding energies. The survey scan is presented in Supporting Information, Figure 4. Quantification of material was carried out by integrating the signals in the survey spectrum and using sensitivity factors for the levels selected for analysis. The binding energies were referenced to the C1s signal of adventitious carbon at 284.8 eV. The C1s signal shows a carboxylate signal at 288.8 eV in addition to a main signal centered at 284.8 eV. The N1s region of the spectrum contains a single N1s signal at 400.3 eV, consistent with nitrogen atoms in polymer structure. The high-resolution spectrum for the signals Pd3d gave a binding energy of 335.3 eV, associated with the position of Pd (Supporting Information, Figure 4C). Finally, the O1s region contains a major signal at 532.1 eV and a minor signal at 530.3 eV. There was an overlap with the Pd3p3 signal at this region. The former signal is associated with oxygen in contact with carbon atoms, and the latter is associated with an inorganic oxide (more likely PdO). The composition of the PAA-Pd measured yielded 69.5% C 1s, 8.2% N 1s, 8.6% O 2s, and 13.7% Pd3d. Supporting Information, Figure 4 B showed that even after dispersion of PdNPs in PAA the oxidation state of PdNPs was zero with a binding energy of 535.3 eV ($3d_{5/2}$).[32]

Reduction of Cr(VI) by Polyamic Acid. PAAs can be considered as polyfunctional materials in terms of amide and carbonyl functionalities. An average functionality can vary from 160 to 600 depending upon its molecular weight. Any reactive materials having two or more functionalities can cross-link the PAA to produce a high molecular weight cross-linked polymeric network. PAA is a precursor of polyimides with cation complexing properties.[29−31] It is believed that the complexing power of PAA is significantly higher than that of the imide form, implying the ability of the carboxylic acid groups to exhibit polyfunctional behavior. Moreover, the possibility of creating monodispersed, nanoscale particles of noble metals can be used to create a high density of anchor groups for directed immobilization of Cr(VI). Different amounts of the chemically synthesized polyamic acid were added to 10.0 mL of Cr(VI) solutions at different concentrations. The reaction, which was carried out at varying times, was followed by filtration and separation of polyamic acid particles. In

the presence of a metallic salt, the negatively charged polycarboxylate couples to metal cation forming metal-carboxylate salt (polyamate)-COOCr groups in PAA. The neutral form of polyamic acid is oxidized to an electron deficient species (PAA^+) with simultaneous reduction of Cr(VI) in solution as outlined in eqs 2−4:[33]

$$3PAA^{o} \rightarrow 3PAA^{+} + 3e^{-} \quad (2)$$

$$CrO_4^{2-}(aq) + 8H^{+} + 3e^{-} \rightarrow Cr^{3+}(aq) + 4H_2O(l) \quad (3)$$

$$CrO_4^{2-}(aq) + 3PAA^{0}(s) + 8H^{+} \rightarrow Cr^{3+}(aq) + 3PAA^{+}(s) + 4H_2O(l) \quad (4)$$

Using spectrophotometric techniques, the concentration of Cr(VI) in solution was determined before and after exposure to (i) the PAA powder, (ii) PAA powder and PdNPs, and (iii) PAA powder and PdNPs raised above ambient temperatures. As shown in Figure 2, the amount of PAA added to the Cr(VI) solution directly influences the efficiency of Cr(VI) to Cr(III). It was also noted that the amount of PAA needed to efficiently reduce Cr(VI) depends on the initial concentration of the Cr(VI) solution.

To obtain the optimum amount of PAA needed to effectively reduce Cr(VI), various amounts (0.25 to 2.00 mg) of PAA were added to a 10 mL solution of 0.5 μM Cr(VI). The extent of reduction was monitored after 14 min of exposure to PAA (Figure 3 A). The experiment was repeated in the presence of PAA and 0.5 mg PdNPs and last in1 the presence of PAA and 0.5 mg of PdNPs at 40 °C. It was observed that the application of 1.50 mg of PAA is sufficient to initiate the reduction of Cr(VI) with efficiency higher than 86%. In the presence of PdNPs, the reduction efficiency increased to 90% and a further increase to 100% was recorded when the temperature was changed from ambient to 40 °C. Thus, application of 1.50 mg of PAA for lower concentrations of Cr(VI) solutions and the inclusion of PdNPs with heating drastically increases the reduction efficiency of the system. Different experimental conditions were tested: 0.5 μM of Cr(VI) only, PAA/PdNPs, and PAA/PdNPs/heat) to assess the effect of PAA in both the absence and the presence of PdNPs.

As shown in Figure 3B and C, without PAA, no reduction in Cr(VI) is observed even in the presence of PdNPs at both ambient and elevated temperatures. This supports the idea that the polymer provides the necessary electrons to reduce the metal ions. In the presence of PAA, Cr(VI) was reduced by 22% after the first minute while at 70% reduction was recorded after 5 min exposure. At 14 min exposure time, the reduction efficiency increased to 89%. It was noted that the reduction of Cr(VI) is significantly accelerated in the presence of PdNPs since 36% reduction is recorded after the first minute whereas 77% of Cr(VI) reduction occurred after 5 min. At 14 min reaction time, the reduction efficiency increased to 95%. Change in the energetics of the reaction was studied by changing the temperature of the system from ambient to 50 °C and observing the UV−vis absorption peaks at 350 nm of the resulting residual Cr(VI) at intervals of 5 °C.[4] The absorption peaks completely diminished at 40 °C indicating that the efficiency of Cr(VI) reduction by the PAA/PdNPs composite is optimal at this temperature. First order exponential decay fit gave R^2 values ranging from 0.981

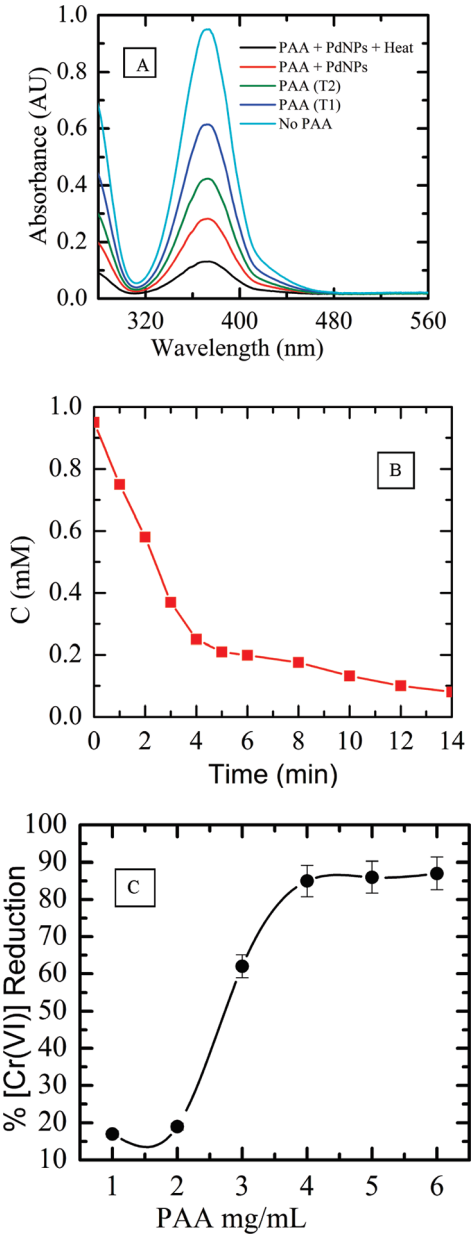

Figure 2. (A) Cr(VI) reduction by PAA, PAA in the presence of PdNPs at two different temperatures (T_1 = 25 ± 0.5 °C and T_2 = 30 ± 0.5 °C) and PAA in the presence of PdNPs at 40 ± 0.5 °C. (B) The changes in the concentration of Cr(VI) with time during exposure to PAA. (C) The efficiency in the Cr(VI) reduction with the initial concentration of 0.500 μM during exposure to 1.0−6.5 mg/mL of PAA.

to 0.990 as shown in Figure 3 B. It has previously been reported that reduction of Cr(VI) was a first order reaction with respect to reductants such as formic acid/sulfur nanoparticle composite and 1-butanol in micellar media[1,2,34]

Optimum Reduction Time. Further experiments were carried out to evaluate the optimum time needed to significantly reduce the solutions of Cr(VI). Consequently, different initial concentrations of Cr(VI) solutions in the range of 1−150 mM were exposed to the same amount (1.5 mg) of PAA. The concentration of Cr(VI) after exposure to PAA powder versus its initial concentration (C_t/C_0) was plotted against time (Supporting Information, Figure 5). Results showed that the

dx.doi.org/10.1021/cs100034z |ACS Catal. 2011, 1, 139–146

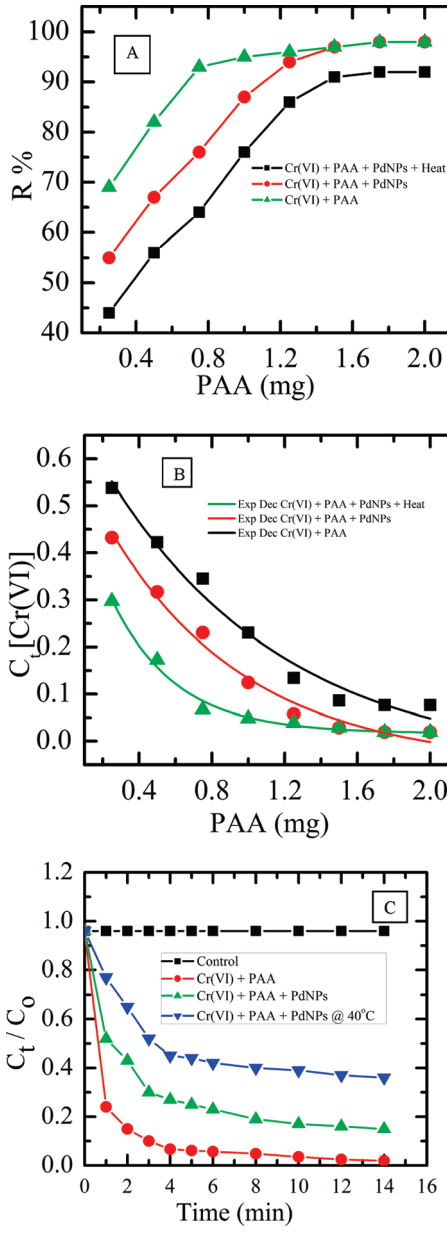

Figure 3. (A) Progressive % reduction efficiency profile of 10 mL of Cr(VI) solution with an initial concentration of 0.5 μM using different amounts (0.25 to 2.00 mg) of polyamic after 14 min of exposure at 40 °C. (B) Exponential decay plot of Cr(VI) reduction at different conditions. (C) Cr(VI) reduction profile in the absence and presence of PAA, PdNPs at both ambient and elevated temperatures.

reduction efficiency increased by increasing the treatment time and that an exposure time of 15 min is necessary to achieve a reduction efficiency of 96.6% Cr(VI).

Effect of Initial Concentration of Cr(VI). Further experiments were carried out to evaluate the ability of PAA to reduce Cr(VI) solutions at various initial concentrations. Results showed that 1.5 mg PAA can be used to reduce 10 mL of Cr(VI) solutions in the concentration range of 1.0×10^{-1}—1.0×10^{2} mM with reduction efficiencies at 99.9%. However, in Cr(VI) solutions with the concentrations higher than 1×10^{5} μM, the reduction efficiency decreased as expected by 19.9%. PAA can thus be used to reduce toxic Cr(VI) at neutral media (pH 7.0) within the concentration range of 1.0×10^{-1}—1.0×10^{2} mM. (Figure 6 in Supporting Information).

Reduction of Hexavalent Chromium at PAA-Modified Gold Electrode. As stated earlier, the reduction of Cr(VI) to Cr (III) using PAA was carried out in both the solution phase and at solid gold electrodes. The response of various Cr(VI) concentrations to the PAA-modified Au-electrode was evaluated using cyclic voltammetry at PAA-modified and bare Au-electrodes. By running CV (10 and 15 cycles) in acetate buffer (pH 5) to confirm PAA stability, results showed stable characteristic of PAA signals with oxidation and reduction peaks observed (Supporting Information, Figure 2). Figure 4 A and B shows the voltammograms recorded at varying concentrations of Cr(VI) (50—1000 μM) in acetate buffer (pH 5.0). At very low concentration of Cr(VI) 50 μM, both oxidation and reduction peaks were observed whereas at high concentration of Cr(VI) 1000 μM, the reaction showed the presence of a reduction peak and absence of an oxidation peak according to eq 2—4.

The control reaction consists of a solution of acetate buffer (pH 5.00) showing a well-defined reduction peak at +208 mV on bare gold electrode (Figure 4 A). The presence PAA film on the electrode surfaces causes the oxidation peak to diminish through an irreversible reduction of Cr(VI). Compared to the control, it was noted that PAA produced a peak at +595 mV that is attributed to Cr(VI). As the concentration of Cr(VI) decreased, the redox peak heights diminished as a function of Cr(VI) concentration (Figure 4 B). This indicates the ability of PAA-modified Au-electrode to act as a surface for the reduction of Cr(VI) to Cr(III). The reversible switching between oxidized and reduced forms of the PAA by electrochemical doping/undoping provides a means for repetitive and reusable reduction of Cr(VI) in complex media (eq 4).

Aliquots from the reaction mixture were periodically removed from the electrochemical cell and the resulting concentration determined on an HP 8453 UV—visible diode array spectrophotometer. Using the electrochemical reduction, the efficiency of 72.84% was recorded in the presence of 114 mg/mL of PAA. This is significant as most methods of Cr(VI) remediation such as the biosorption of Cr(VI) take 2 h to produce 86% reduction. Thus, the PAA reduction approach is viable in the effective reduction of Cr(VI) to Cr(III).

Confirmation of Cr(III) as the Reaction Product. The presence of Cr(III) as the reaction product was confirmed using both colorimetric and EPR techniques. When excess of sodium hydroxide solution was added to a solution of the products obtained following the reduction Cr(VI) with PAA and PdNPs, a green solution was observed. The free Cr(III) ions reacted with excess sodium hydroxide solution to produce the green hexahydroxochromate (III) solution.[35] Further confirmation was carried out by warming the resulting solution with hydrogen peroxide solution (oxidation), which produced a bright yellow solution containing Cr(VI) ions (this step reversed the reaction back to Cr(VI).

Additional confirmation was carried out using EPR, since the formation of the greenish-Cr(III) solution is prone to interference by similarly colored iron(II) salts. EPR can distinguish Cr(III) from other complexes by monitoring its paramagnetic behavior since Cr(III) has a d^3 electronic configuration with half filled t_{2g} orbitals. Results for EPR analysis of the product confirmed that the product of reaction occurring between Cr(VI), PAA, and PdNPs at 40 °C is indeed Cr(III) Figure 5.

dx.doi.org/10.1021/cs100034z |ACS Catal. 2011, 1, 139–146

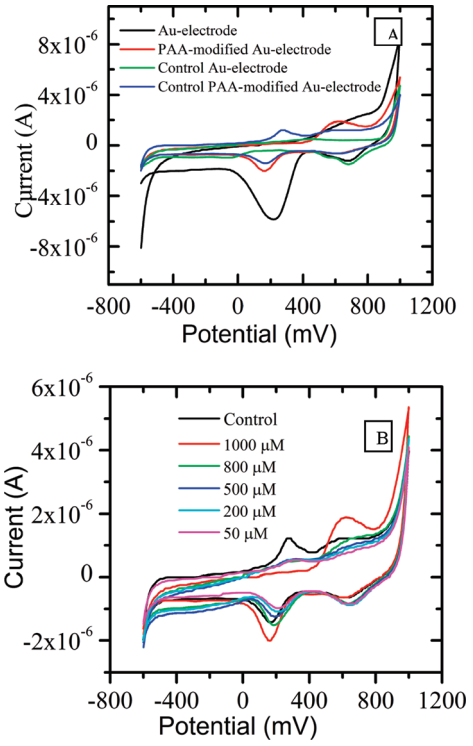

Figure 4. [A] Cyclic voltammetric response on a PAA-modified and unmodified Au-electrode in 0.1 M acetate buffer (pH 5.0) and 50 μM Cr(VI). [B] Cyclic voltammetric response on a PAA-modified Au-electrode at varying concentrations of Cr(VI) (50−1000 μM) in 0.1 M acetate buffer (pH 5.0).

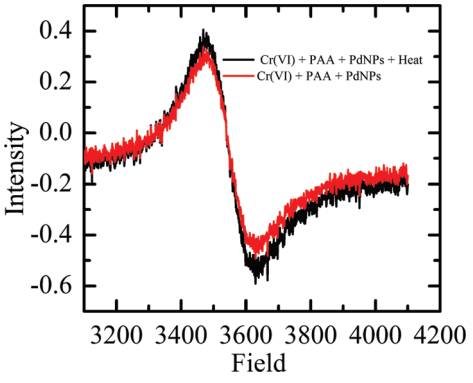

Figure 5. EPR spectra of Cr(III) after reduction of Cr(VI) with PAA in the presence and absence of PdNPs.

CONCLUSIONS

Production of different sizes of palladium nanoparticles (3−20 nm in diameter) have been achieved using different amounts of $NaBH_4$. After and before dispersion in PAA, the PdNPs had oxidation state zero with a binding energy of 335.3 eV. The generated PdNPs were consequently used to catalyze the reduction of Cr(VI) using PAA. The two forms of PAA, namely, the powder and the film on a Au-electrode were used for the reduction of highly toxic Cr(VI) to the benign Cr(III) which was confirmed using the EPR technique. The effects of various parameters such as palladium nanoparticles as catalyst and initial Cr(VI) concentration on the kinetics and efficiency of reduction process were investigated. The use of palladium nanoparticles at ambient temperatures increased the reduction efficiency to 90.2% and a further increase to 99.9% reduction efficiency at 40 °C within 14 min. This is significant as methods of Cr(VI) remediation such as the biosorption of Cr(VI) and bacterial degradations take 2 h to produce 86% reduction and sometimes days. Thus, the PAA reduction approach is viable in the effective reduction of Cr(VI) to Cr(III).

ASSOCIATED CONTENT

Supporting Information. Schematics of Cr(VI) ions reduction by poly(amic acid) and formation of the PAA-Cr(III) complex, graphs showing the residual Cr(VI) plotted against exposure time, the reduction efficiency of Cr(VI) in solution at different initial concentrations ($10-10^7$ μM) using 1.5 mg of PAA powder within 15 min of exposure. CV of PAA-modified Au-electrode, XRD and XPS characterization of PdNPs before and after dispersion in PAA. TEM images of PdNPs. These materials are available free of charge via the Internet at http://pubs.acs.org.

AUTHOR INFORMATION

Corresponding Author

*E-mail:osadik@binghamton.edu. Fax: (607)777-4478.

Funding Sources

This material is based on work partially supported by the IGERT Program of the National Science Foundation under Agreement no. DGE-0654112, administered by the Nanobiotechnology Center at Cornell. U.S.-EPA is also acknowledged through the STAR funding.

ACKNOWLEDGMENT

We acknowledge Dr. David Doetschman for EPR analysis and Dr. Anju Sharma for XPS analysis.

REFERENCES

(1) Omole, M. A.; K'Owino, I. O.; Sadik, O. A. *Appl. Catal., B* **2007**, *76*, 158–167.

(2) K'Owino, I. O.; Omole, M. A.; Sadik, O. A. *J. Environ. Monit.* **2007**, *9*, 657–665.

(3) Omole, M. A.; Kowino, I. O.; Sadik, O. A. In *Nanotechnology Applications: Solutions for Improving Water Quality*; Street, A., Duncan, J., Mamadou, D., Savage, N., Sustich, R., Eds.; EPA Handbook on Nanotechnology, **2009**.

(4) Code of Federal Regulation. Protection of Environment. Section 141. 80, Title 40, p 425.

(5) Zachara, J. M.; Ainsworth, C. C.; Brown JR, E. G.; Catalano, G. J.; Mckinley, P. J.; Qafoku, O.; Smith, C. S.; Szecsody, E. J.; Traina, J. S.; Warner, A. J . *Geochim. Cosmochim. Acta* **2004**, *68*, 13–30.

(6) Sylvester, P.; Rutherford, A. L.; Gonzalez-Martin, A.; Kim, J. *Environ. Sci. Technol.* **2001**, *35*, 216–221.

(7) Patterson, J. W. *Industrial wastewater treatment technology*, 2nd ed.; Butterworth publishers: Boston,1985.

(8) Fabiani, C.; Ruscio, F.; Spadoni, M.; Pizzichini, M. *Desalination* **1997**, *10*, 183–191.

(9) Ludvik, J. United Nations Industrial Development, 2000, US/RAS/92/120/11-51.

(10) Wei, C.; German, S.; Basak, S.; Rajeshwar, K. *J. Electrochem. Soc.* **1993**, *140*, L60–L62.

(11) Alfonso, D. R.; Cugini, A. V.; Sorescu, D. C. *Catal. Today* **2005**, *99*, 315–322.

(12) Ruotolo, L. A. M.; Gubulin, J. C. *React. Funct. Polym.* **2005**, *62*, 141–151.
(13) Senthurchelvan, R.; Wang, Y.; Basak, S.; Rajeshwar, K. *J. Electrochem. Soc.* **1996**, *143*, 44–51.
(14) Ruotolo, L. A. M.; Gubulin, J. C. *Chem. Eng. J.* **2005**, *110*, 113–121.
(15) Farrell, S. T.; Breslin, C. B. *Environ. Sci. Technol.* **2004**, *38*, 4671–4676.
(16) Olad, A.; Nabavi, R. *J. Hazard. Mater.* **2007**, *147*, 845–851.
(17) Danilov, F. I.; Protsenko, V. S. *Russ. J. Electrochem.* **1998**, *34*, 276–281.
(18) Faldini, S. B.; Agostinho, S. M. L.; Chagas, H. C. *J. Electroanal. Chem.* **1990**, *284*, 173–183.
(19) Cox, A. J.; Kulesza, J. P.; Mbugwa, A. M. *Anal. Chem.* **1982**, *54*, 787–789.
(20) Cox, J. A.; Kulesza, P. J. *Anal. Chim. Acta* **1983**, *154*, 71–78.
(21) Paneli, M.; Voulgaropoulos, A. V.; Kalcher, K. *Mikrochim. Acta* **1993**, *110*, 205–215.
(22) Turyan, I.; Mandler, D. *Anal. Chem.* **1997**, *69*, 894–897.
(23) Ge, H.; Zhang, J.; Wallace, G. G. *Anal. Lett.* **1992**, *25*, 429–441.
(24) Sittig, M. *Handbook of toxic and hazardous chemicals*, 3rd ed.; Noyes Publications: Park Ridge, NJ, 1991; p 840.
(25) Andreescu, D.; Wanekaya, A. K.; Sadik, O. A.; Wang, J. *Langmuir* **2005**, *21*, 6891–6899.
(26) Du, N.; Wong, C.; Feurstein, M.; Sadik, A. O. *Langmuir* **2010**, *26*, 14194–14202.
(27) Wang, W.; Efrima, S.; Regev, O. *Langmuir* **1998**, *14*, 602–610.
(28) Ramirez, E.; Jansat, S.; Philippot, K.; Lecante, P.; Gomez, M.; Masdeu-Bultó, A. M.; Chaudret, B. *J. Organomet. Chem.* **2004**, *689*, 4601–4610.
(29) Linde, H. G. *J. Appl. Polym. Sci.* **1990**, *40*, 2049–2063. (b) Schoch, K.; Su, W.-F. A.; Burke, M. *Langmuir* **1993**, *9*, 278–283.
(30) Gniewek, A.; Ziolkowski, J. J.; Trzeciak, A. M.; Kepinski, L. *J. Catal.* **2006**, *239*, 272–281.
(31) Kakimoto, M.; Suzuki, T.; Konishi, T.; Imai, Y.; Iwamoto; Hino, T. *Chem. Lett.* **1986**, 823–826.
(32) Nefedovm, V. I.; Salyn, Y. V.; Moiseev, I. I.; Sadovskii., A. P.; Berenbljum., A. S.; K Nizhnik., A. G.; Mund, S. L. *Inorg. Chim. Acta* **1979**, *35*, 343.
(33) Tian, Y.; Yang, F. L. *J. Cleaner Prod.* **2007**, *15*, 1415–1418.
(34) Basu, A.; Saha, B. *Am. J. Anal. Chem.* **2010**, *1*, 25–30.
(35) Abass, E.; Alireza, M. N.; Reza, V. *Am. J. Appl. Sci.* **2005**, 1471–1473.